

Energy Management Control Strategy Based on Harris Hawks Optimization Technique for Fuel Cell Hybrid Electric Vehicle [†]

Gondu Vykunta Rao ^{1,*}, Ankit Soni ², Aruna Bharathi ³, Baratham Murali ⁴ and Vanjarapu Vykunta Rao ⁵

¹ Core Engineering, Work Integrated Learning Programmes, Division, Birla Institute of Science & Technology, Deemed University, Vidya Vihar, Pilani 333031, India

² Automotive Electronics, Work Integrated Learning Programmes, Division, Birla Institute of Science & Technology, Deemed University, Vidya Vihar, Pilani 333031, India; 2021ht65136@wilp.bits-pilani.ac.in

³ Electrical and Electronics Department, Geethanjali College of Engineering and Technology, Hyderabad 501301, India; arunabharathi916@gmail.com

⁴ Electrical and Electronics Department, Miracle Educational Society Group of Institutions, Vizianagaram 535216, India; muralibaratam4@gmail.com

⁵ Electrical and Electronics Department, Sri Venkateshwara College of Engineering and Technology, Srikakulam 532410, India; vykuntabits@gmail.com

* Correspondence: vykunta.rao@wilp.bits-pilani.ac.in; Tel.: +91-741-619-6828

[†] Presented at the International Conference on Recent Advances in Science and Engineering, Dubai, United Arab Emirates, 4–5 October 2023.

Abstract: The focus and sales of EVs are slowly coming into scope, as the power source of such vehicles is a significant area in which the integration of power systems is becoming a crucial issue. This work involves the use of hybrid sources, batteries as a primary source, fuel cells, and an ultra-capacitor as an auxiliary source. This hybrid system provides the grip of the FCEV. The constraints of fuel cells are the SOC of the battery and the H₂ level. These three power sources in hybrid systems are connected to the DC bus via proper DC-to-DC converters. This paper will discuss the combination of Harris Hawks Optimization (HHO) for the energy management and control of these source systems, for the constraint of mandated sources, and to ensure stability. The proposed system provides a satisfactory energy management system for the hybrid system. Using the proposed technique, the fuel consumption settling period is reduced. The proposed method was implemented and validated with and without the HHO technique.

Keywords: electric vehicles; battery; fuel cell; ultra-capacitor; solar; Harris Hawks Optimization HHO technique



Citation: Rao, G.V.; Soni, A.; Bharathi, A.; Murali, B.; Rao, V.V. Energy Management Control Strategy Based on Harris Hawks Optimization Technique for Fuel Cell Hybrid Electric Vehicle. *Eng. Proc.* **2023**, *59*, 206. <https://doi.org/10.3390/engproc2023059206>

Academic Editors: Nithesh Naik, Rajiv Selvam, Pavan Hiremath, Suhas Kowshik CS and Ritesh Ramakrishna Bhat

Published: 23 January 2024



Copyright: © 2024 by the authors. Licensee MDPI, Basel, Switzerland. This article is an open access article distributed under the terms and conditions of the Creative Commons Attribution (CC BY) license (<https://creativecommons.org/licenses/by/4.0/>).

1. Question of Research

Power sources are a primary concern in EVs. Why are only batteries used as power sources, why can other sources not be used, and why are sources not integrated? Refs. [1–3].

2. Introduction

New hydrogen technology is rapidly emerging for electric vehicle propulsion systems. Fuel cell systems (FCSs) will play an important role in electric vehicles in the coming decades. This energy source has many advantages, from the environment to its efficiency and effectiveness [4]. Because the power response of FCSs is small, PEMFC (proton exchange membrane fuel cell)-powered vehicles may become unstable during sudden load changes.

An energy management system (EMS) is needed to produce the power from the hybrid source to distribute the load. EMSs meet the hybrid resource constraints used to achieve the high recital of the projected method and improve the fuel economy [5–7]. Rule-based control and optimization-based control techniques are used in some of the literature. These

often have success or reverse the cycle. Ideally, a reduction in hybrid fuel consumption can only be achieved when driving conditions are known to be necessary.

PMEFCs can provide non-stop energy to electric vehicles. As a result, hydrogen-powered PEMFCs are used [8]. This is the best power source and removes conventional fossil fuel usage. Battery (BT)-powered devices and Ultra-capacitors (UCs) are known for their high power. BTs can provide long-term alternative energy. (UCs) are also used to control the energy compared to the battery. The efficiency and power of UCs are high, and their discharging and charging cycles are also increased [9].

Of the hybrid sources that exist, one of the sources is UCs. UCs are electrochemical condenser devices that deliver a very short period of maximum power. UCs consist of an electric motor coated as a double layer. The double coated layer is made up of non-ferrous metals [10–12]. An electric motor is a combination of a power source and an engine. Methanol and propane create hydrogen gas through biological processes and the transformation of hydrocarbons. Designing an EMS system consists of the use of hybrid seeds to manage the power required. The proposed EMS is used to provide and improve the electrical load. The hybrid system provides the grip of the fuel cell EV. The fuel cell constraints are the SOC of the battery and the H_2 level. This work selected PI-based HHO control for energy management. This is used to manage and control the energy, consider the multi-source for source limitation, and improve the system's performance [13]. The workflow of the entire proposed work is described below:

Step 1: The modelling of the battery and analysis of the battery output with/without the HHO technique.

Step 2: The modelling of the fuel cell and analysis of the output with/without the HHO technique.

Step 3: The modelling of the ultra-capacitor and analysis of the output with/without the HHO technique.

Step 4: The integration of the above three sources to see the output of the energy management system for the hybrid system as a whole.

3. Functional Block Diagram of EMS of Fuel Cell Hybrid Electric Vehicle

EMSs (Energy Management Systems) are required by hybrid vehicle systems to achieve good efficiency and performance. According to some control objectives, they determine the energy separation between the system's different energy sources, considering each source's characteristics.

Figure 1 shows that the primary source is a battery, whereas fuel cells and ultra-capacitors are used as supplementary sources. A unidirectional DC/DC converter connects the FC and DC bus to improve the voltage. An ultra-capacitor connects the DC bus using a bidirectional DC/DC converter for charging and discharging, and is connected to the DC bus for maintaining bus voltage.

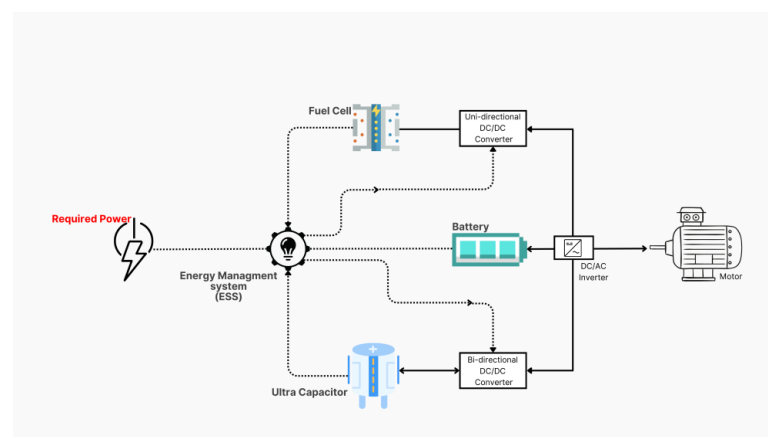


Figure 1. Block diagram representation for proposed HHO system.

4. Battery Modelling and Analysis

A model of a dynamic equivalent circuit. The diagram in Figure 2 suggests the simulation study. The simulation circuit comprises a direct current voltage source, a series resistance, and two RC parallel circuits. The DC voltage source represents the battery's open circuit voltage in series networks. R_s denotes the internal DC resistance and the RC parallel denotes the networks, which characterize the transient response of the voltage and current V_t . The rate capacity effect is also deliberated in this model, where the usable capacity is varied, with the current representing the terminal voltage. The SOC of the battery is calculated based on the value of the functional capacity parameters depending on the SOC and current.

$$V_t = OCV - V_1 - V_2 - V_s \tag{1}$$

$$V_s = I \times R_s \tag{2}$$

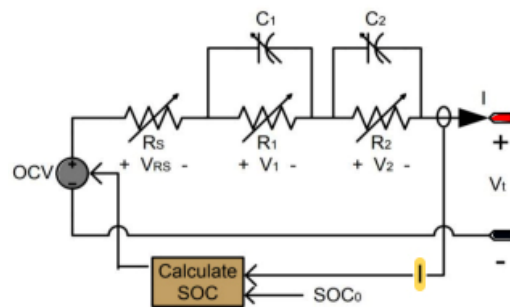


Figure 2. Equivalent circuit model of battery.

The battery open circuit voltage is denoted as $V_{oc\ BAT}$, the battery's output voltage is denoted V_{BAT} , and the battery series resistance is represented as R series. The R-C circuit is multiple time constants for the circuit designed. They are τ -hour, τ -sec and τ -min. These parameters are called SOC functions and are also used to model the transient behavior of the battery. The battery state of charge calculation is performed using the following equation.

5. Survey and Case Studies

Migration towards electric vehicles has started globally in India, and the significant adoption of these vehicles began in 2021. The prime reason for accepting these vehicles could be the exorbitant increases in the price of fossil fuel in the past few years. The alternate solution product, the electric vehicle rung cost, is deficient compared to the currently available products.

Comparative study of various types of fossil fuel alongside alternate fuel technology (CNG and EV) vehicles to understand the running cost per km and the cost of ownership of these vehicles.

$$SOC = SOC_0 + \frac{\eta_{BAT}}{(3600 \cdot C_{BAT})} \int i_{BAT} dt \tag{3}$$

where the battery's initial parameters are i_{BAT} & SOC_0 is the battery's initial current and sate of charge, and C_{BAT} is the battery's capacity.

6. Fuel Modelling and Considerations

As show in the Figure 3, the fuel cell is a type of battery that uses hydrogen and oxygen as fuel. It converts chemical energy directly into electrical energy through an electrode reaction. A simplified model for the fuel cell has been established.

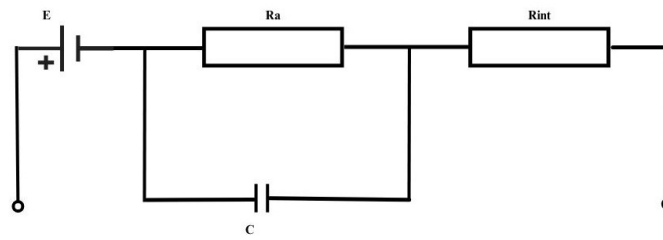


Figure 3. Equivalent circuit model of fuel cell.

When the load current changes due to the charging effect, the fuel cell generates a gradually changing voltage on the bipolar plate surface. This voltage is accompanied by an equivalent resistance R_a , which is connected in parallel with a capacitor C , as shown in the given diagram of a specific equivalent model.

$$[E_{cell} - R \cdot j_{Stack} - A \cdot \ln(j_{Stack} + j_l) - m \exp(n j_{Stack})] (j_{Stack} = I_{Stack} / A_{cell}) \tag{4}$$

where V_{FC} is the fuel cell voltage; i_{FC} is the current for the fuel cell; A_{cell} is each fuel area; E_{cell} is the fuel cell reversible voltage; N is the fuel cell stack number; j_{stack} is the density of the FC current; R is the specific resistance of the membrane area; m and n are the two mass transfer coefficients; A is the coefficient of T ; α , β and γ are second-order model approximating coefficients; I_{stack} is the fuel stack current; and i_{FC} is the output current of the fuel cell.

7. Ultra-Capacitor Modelling and Consideration

A fuel cell is a device that uses hydrogen and oxygen as fuel through an electrode reaction that directly converts chemical energy into electrical energy. At present, a simplified model concerning the model has been established.

When the load current changes due to the fuel cell’s bipolar plate surface, it produces a slow charging effect in response to the charging effect. The voltage is being changed. The corresponding resistance R_a is linked in parallel with a capacitor C , as shown in the specific equivalent model diagram of the capacitor C which is represented in the Figure 4.

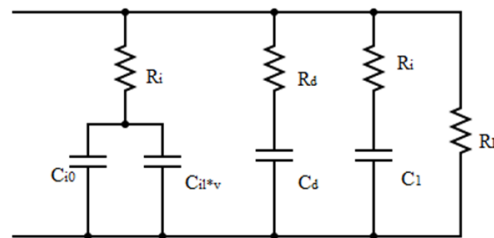


Figure 4. Equivalent circuit model of supercapacitor.

8. Design and Implementation of EMS Controller

8.1. Proportional Term

The proportional time produces an output value proportional to the current error value. The proportional response can be modified by multiplying the error by a constant K_p , called the proportional gain constant. The proportional term is given by the following:

$$P_{out} = K_p e(t) \tag{5}$$

A high proportional increase causes a significant change in the output for a given change in error. If the proportional increase is too high, the system can become unstable. In contrast, a slight gain results in a small output for a significant input error, and the controller is unresponsive or less responsive. If the gain balance is too low, the control will be too

small when responding to internal disturbances. Tuning theory and industrial practice show that the proportional time should contribute to the number of output changes.

8.2. Integral Term

The contribution from the critical point is proportional to both the magnitude of the error and the duration of the error. The key in the PID controller is the number of instantaneous errors over time and provides variables that must be corrected in the past. The excess error is divided by the gain (K_i) and added to the output. The main point is given by the following:

$$I_{out} = K_i \int_0^t e(T)dT \tag{6}$$

The movement of the process is performed by the integral term toward the set point and eliminates the residual steady-state error that occurs with a pure proportional controller. However, since the central term corresponds to accumulated errors from the past, it can cause the current value to exceed the set point value. Which, the complete working block diagram representation in Figure 5.

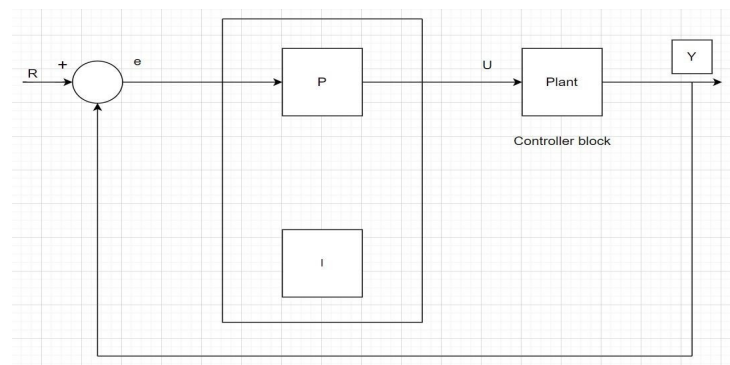


Figure 5. Block diagram representation of PI controller.

The PI controller can guarantee a fast response due to proportional action, and the integral action will make the steady-state error zero by adequately selecting the parameters K_c and T_i values. If the error is zero, the previous value of the integral term is retained as an output signal. When the error changes from zero, the proportional term works for correction, and the integral term increases or reduces the output.

9. Implementation of HHO for the Proposed Application

The converter’s switching pulse is generated using the Harris Hawks Optimization technique in a closed-loop operation. Here, the error signal is given to the PI controller. The PI Controller controls the error signal. So, this error signal is considered an objective function problem.

Mathematically, this can be represented as follows:

$$P = K_p e_p(t) + K_p K_I \int_0^T e_p(\tau)d + P_I(0) \tag{7}$$

where

P = PI controller’s output

K_p = Proportional gain

K_I = Integral gain

(t) = Desired value of controlled variable—measured value

(0) = Integral term initial value.

The proposed optimization techniques take this error signal as an objective function.

The tuning of the parameter problem is formulated as an optimization problem, and to identify the optimal, it is applied. The controller parameters have to be tuned

for satisfactory plant operations. The objective of the optimization problem is to reduce hydrogen consumption and achieve a quick settling. The figure below shows the flowchart of the tuned PI controller. The following issues must be addressed while applying the HHO for any problem. The same represented in the Figure 6. Tuning of PI controller using HHO.

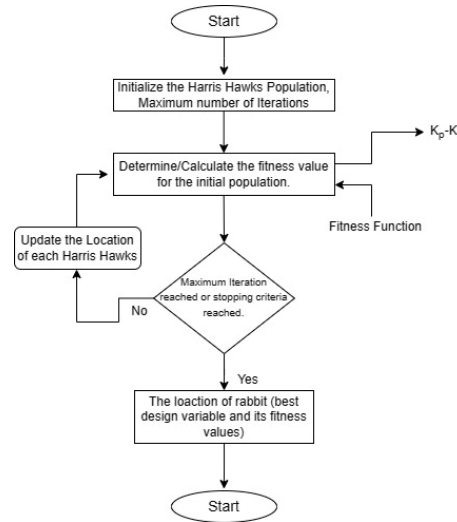


Figure 6. Tuning of PI controller using HHO.

Step_1: The individual population represents the parameters of the PI.

Step_2: HHO searches for the optimal solution by maximizing the fitness function and, therefore, an evaluation function that measures the quality of the problem solution.

Step_3: In the transmission line voltage control process, in terms of the system time constant, the objective is to minimize the Integral Square Error (ISE), which decides the performance of the transmission line. For removing the negative error component controllers, the ISE squares the error to remove.

$$ISE = \int_0^T e^2(t)dt \tag{8}$$

Step_4: HHO minimizes the fitness function, and the minimization objective function is transformed into the fitness function = 1/ISE. The ISE is used as the basis of the fitness function. The HHO, however, maximizes the fitness function, whereas the ISE needs to be minimized. The same mentioned in the Table 1.

Table 1. The parameters considered for HHO optimizers.

Sl.No	Parameter Type	Value Considers
1	Maximum iteration	500
2	Number of Hawks	30

For the compensation process, K_p and K_i are the control parameters.

Where

$$K_i = K_p / \tau_i \tag{9}$$

The considered parameters for PI are as follows:

$$0.1 < K_i < 1$$

$$1 < K_p < 3$$

10. Implementation of the Proposed System

The proposed system was simulated and implemented in MATLAB/Simulink. A controlled voltage source represents the terminal voltage V_{ocv} of the battery. At the same

time, five subsystems control the voltage value of the battery model: SOC calculation, OCV calculation, RC values, voltages of RC parallel networks, and VRS. The I measurement produces the current value for the subsystems. SOC₀ represents the initial SOC, whereas SOC_n represents the real-time SOC_n.

Figure 7a,b shows the boost converter obtaining output from the battery. The battery output voltage is DC. The Simulink results are compared without and with the optimization techniques [11–15].

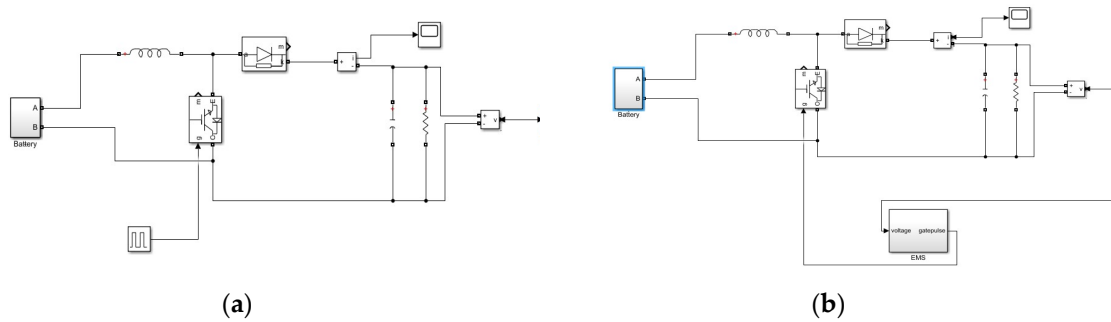


Figure 7. (a) Simulink model without HHO optimization, (b) the Simulink model with HHO optimization.

11. Results and Discussion

From the converter results from the Figures 8 and 9, the proposed optimization techniques produce a constant output voltage, and the rise time is low. Without using the optimization techniques, the switching pulse of the converter is given from the pulse generator. But using the proposed optimization techniques, the PI controller is used to generate the pulse of the converter. Here, the PI controller gain values of K_p and K_i are generated through optimization. The objective function of the integral square error is to control the PI controller gain values. The error values are minimized using the proposed optimization technique. Only optimization techniques generate the gain parameter values in the minimized time. Here, the converter’s output voltage is 60 V DC, and the current is 8.6 A. The obtained gain values using HHO are a K_p of 1 and k_i of 0.65 which are discussed in Table 2.

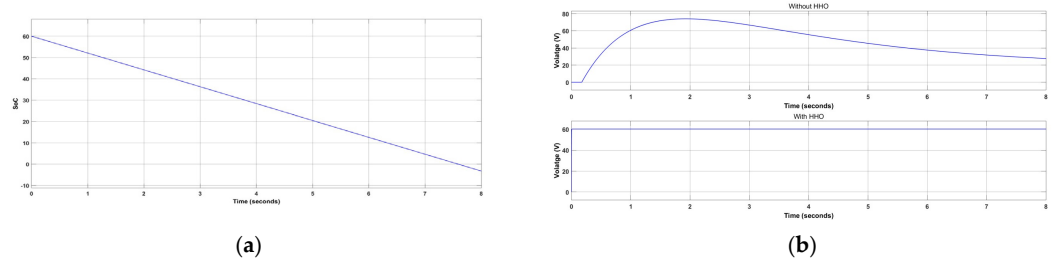


Figure 8. (a) With/without the HHO optimization technique, battery output voltage and SOC; (b) battery output voltage.

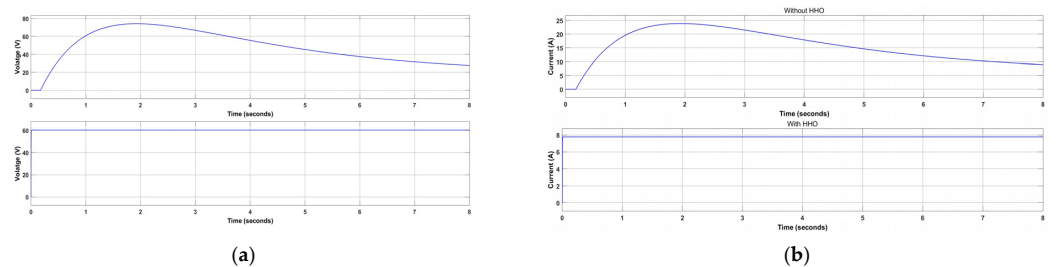


Figure 9. (a) V_{out} of converter, (b) I_{out} of converter.

Table 2. Observations with and without HHO technique implementation.

Sl.No	Parameter Type	Without HHO	With HHO
1	Rise time	0.175	0.001
2	Settling time	1.85	0.005

Results for Integration of the Sources

Figures 10 and 11 shows the proposed multi-source system simulation model created with MATLAB/Simulink. The current measurement block is used to give the present value of the fuel cell, and the voltage measurement block is used to give the voltage value of the FC. The converter obtains output from the multi-source (battery, fuel cell and ultra capacitor). The multi-source system output voltage is DC. The converter fixed the DC voltage to variable DC voltage. The Simulink results are compared to the optimization techniques along with converter specifications used in the design discussed in Table 3.

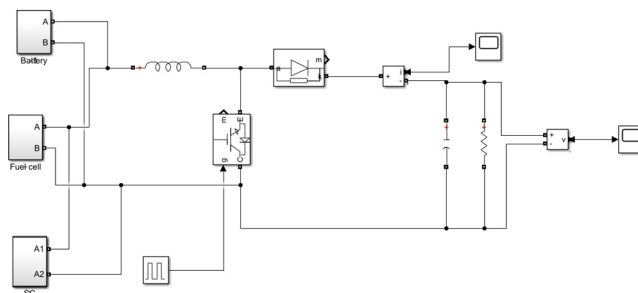


Figure 10. Simulink representation of the integrated multi-source (battery, fuel cell and ultracapacitor).

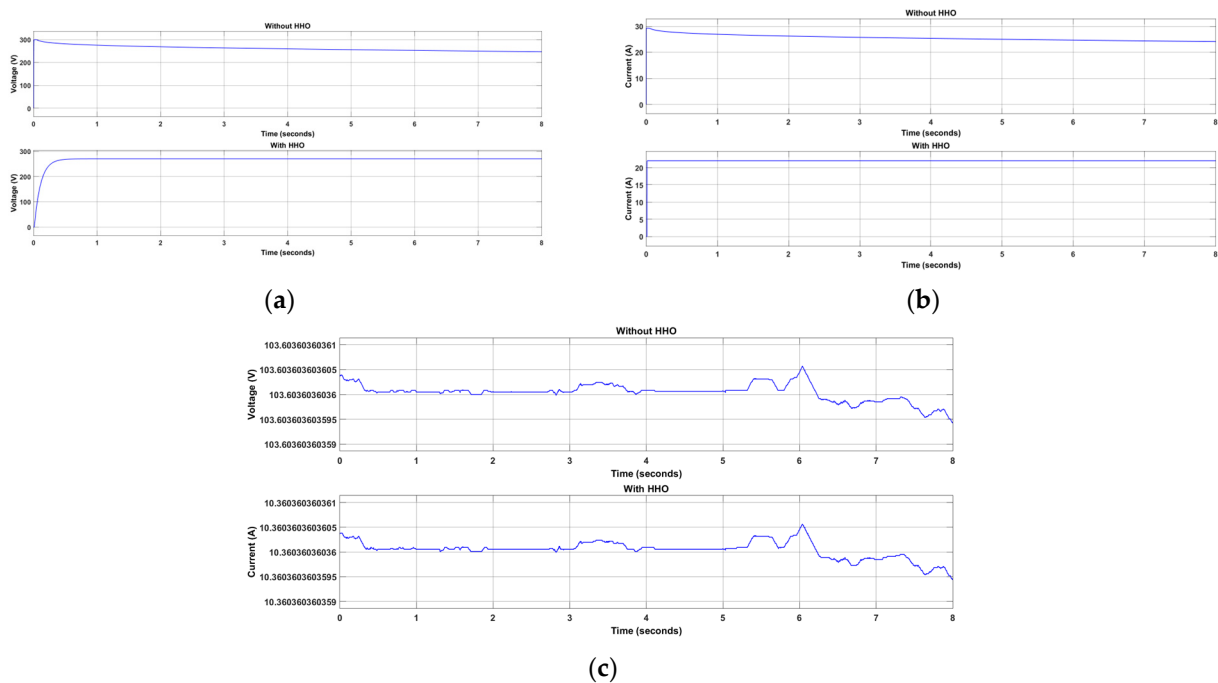


Figure 11. (a) V_{out} of converter, (b) I_{out} of converter. (c) Fuel cell output voltage.

Table 3. Converter design parameters implemented in MATLAB.

Boost Converter	
Parameters	Ratings
Inductance	10 mH
Capacitors	0.1 F
Output inductance	5.5 mH
Output load	1 Ω
Fuel cell voltage	103.6 V
Boost converter voltage of fuel cell	150 V
Battery voltage	3.4 V
Boost the converter voltage of the battery	60 V
Supercapacitor voltage	2.56 V
Boost converter voltage of supercapacitor	60 V

12. Conclusions

The proposed system provides a satisfactory energy management system for the hybrid system. The simulation results under the control of PI-tuned HHO support the validity of the power control strategy. The control strategy is compared by integrating multiple sources (battery, fuel cell, and ultra-capacitor using HHO and without the HHO algorithm). For this comparison, the converter settling time and rise time performance are improved.

Author Contributions: Conceptualization, and methodology, A.S.; software, validation, A.S. and G.V.R.; formal analysis, A.B.; investigation, B.M.; resources, V.V.R.; data curation, G.V.R.; writing—G.V.R. and A.B.; writing—review and editing, G.V.R. and A.S.; visualization, A.S.; supervision, A.B.; project administration, B.M.; funding acquisition, B.M. and V.V.R. All authors have read and agreed to the published version of the manuscript.

Funding: This research received no external funding.

Institutional Review Board Statement: Not applicable.

Informed Consent Statement: Not applicable.

Data Availability Statement: The raw data supporting the conclusions of this article will be made available by the authors on request.

Conflicts of Interest: The authors declare no conflict of interest.

References

- Shrivastava, S.; Swarnkar, P. Comparative study of cell balancing techniques for battery module performance optimization. In Proceedings of the 2023 IEEE International Students' Conference on Electrical, Electronics and Computer Science (SCEECS), Bhopal, India, 18–19 February 2023; pp. 1–6.
- Rao, G.V.; Kumar, S.C.S.; Sivaprasad, A.V.; Sukthana, S.A.; Bharathi, M.A. A Novel Design and Development of Self Maintained Solar Panel. In Proceedings of the 2021 International Conference on Advances in Computing and Communications (ICACC), Kochi, Kakkannad, India, 21–23 October 2021; pp. 1–7. [\[CrossRef\]](#)
- Pattnaik, M.; Badoni, M.; Tatte, Y.; Singh, H. Analysis of electric vehicle battery system. In Proceedings of the 2021 4th International Conference on Recent Developments in Control, Automation & Power Engineering (RDCAPE), Noida, India, 7–8 October 2021; pp. 540–543.
- Rao, G.V.; Bayya, M.; Bharathi, M.A.; Murali, B. A novel design of hybrid EV's based on flux additive DC–DC converter with super capacitor. *J. Physics Conf. Ser.* **2022**, *2327*, 012002. [\[CrossRef\]](#)
- Rao, G.V. Design and development of 1-phase multi-level inverter with power losses calculations. *Int. J. Electr. Eng. Technol.* **2021**, *12*, 80–87. [\[CrossRef\]](#)
- Rao, G.V.; Balamathi, A.; Rajaji, V.D.; Kumar, S.C.S. A Novel Multiple DC-Link with Reduced Switches for Indiscriminate Configuration Single-Phase Switched-Capacitor Multi-Level Inverter. *Des. Eng.* **2021**, *12*, 4911–4922, ISSN: 0011-9342.
- Delizonas, A.; Mademlis, C.; Tsioumas, E.; Papagiannis, D.; Jabbour, N.; Matiakis, T. Low Complexity and High Safety Architecture of Automotive Li-ion Battery Management Systems in Compliance with the ISO 26262 Standard. In Proceedings of the 2023 IEEE International Conference on Electrical Systems for Aircraft, Railway, Ship Propulsion and Road Vehicles & International Transportation Electrification Conference (ESARS-ITEC), Venice, Italy, 29–31 March 2023; pp. 1–6.

8. Rao, G.V.; Chidamparam, P.; Bayya, M.; Bharathi, M.A. A novel design for balancing capacitor voltage of multilevel inverter using space vector pulse width modulation (SVPWM). *Mater. Today Proc.* **2023**, *92*, 1415–1420. [[CrossRef](#)]
9. Rao, G.V.; Bharathi, M.A.; Kumar, S.; Murali, B.; Rao, V.V. Modular battery management system architecture for commercial vehicle applications. *Mater. Today Proc.* **2023**, *92*, 1538–1543. [[CrossRef](#)]
10. ArunaBharathi, M.; Sushama, M.; Venkateswara Rao, K.; Vykunta Rao, G. Experimental and computational analysis of metal oxide nanomaterials for lithium-ion batteries. *Mater. Today Proc.* **2023**, *92*, 1591–1596, ISSN 2214 7853. [[CrossRef](#)]
11. Krishnamoorthy, R.; Kumar, N.; Grebennikov, A.; Ramiah, H. A High-Efficiency Ultra-Broadband Mixed-Mode GaN HEMT Power Amplifier. *IEEE Trans. Circuits Syst. II Express Briefs* **2018**, *65*, 1929–1933. [[CrossRef](#)]
12. Vitee, N.; Ramiah, H.; Mak, P.-I.; Yin, J.; Martins, R.P. A 3.15-mW +16.0-dBm IIP3 22-dB CG Inductively Source Degenerated Balun-LNA Mixer With Integrated Transformer-Based Gate Inductor and IM2 Injection Technique. *IEEE Trans. Very Large Scale Integr. (vlsi) Syst.* **2020**, *28*, 700–713. [[CrossRef](#)]
13. Eswaran, U.; Ramiah, H.; Kanesan, J. Power Amplifier Design Methodologies for Next Generation Wireless Communications. *IETE Tech. Rev.* **2014**, *31*, 241–248. [[CrossRef](#)]
14. Chong, G.; Ramiah, H.; Yin, J.; Rajendran, J.; Wong, W.R.; Mak, P.-I.; Martins, R.P. CMOS Cross-Coupled Differential-Drive Rectifier in Subthreshold Operation for Ambient RF Energy Harvesting—Model and Analysis. *IEEE Trans. Circuits Syst. II Express Briefs* **2019**, *66*, 1942–1946. [[CrossRef](#)]
15. Tan, G.H.; Ramiah, H.; Mak, P.-I.; Martins, R.P. A 0.35-V 520- μ W 2.4-GHz current-bleeding mixer with inductive-gate and forward-body bias, achieving >13-DB conversion gain and >55-DB port-to-port isolation. *IEEE Trans. Microw. Theory Tech.* **2017**, *65*, 1284–1293. [[CrossRef](#)]

Disclaimer/Publisher’s Note: The statements, opinions and data contained in all publications are solely those of the individual author(s) and contributor(s) and not of MDPI and/or the editor(s). MDPI and/or the editor(s) disclaim responsibility for any injury to people or property resulting from any ideas, methods, instructions or products referred to in the content.